J Mater Sci (2009) 44:6805–6810
DOI 10.1007/s10853-009-3572-y

MESOSTRUCTURED MATERIALS

Close-packed array of gold nanoparticles and sum frequency generation spectroscopy in total internal reflection: a platform for studying biomolecules and biosensors

Gérard Tourillon · Laurent Dreesen · Cédric Volcke · Yannick Sartenaer · Paul A. Thiry · André Peremans

Received: 14 October 2008 / Accepted: 12 May 2009 / Published online: 28 May 2009

Abstract An approach is introduced for studying the adsorption and recognition mechanisms of biomolecules, without using any markers. We show for the first time, that the sum frequency generation spectroscopy performed in the total internal reflection (TIR-SFG) geometry, combined with a regular close-packed array of gold nanoparticles allows to probe with a high sensitivity the changes in conformation and orientation induced by the recognition process of avidin by biocytin. This approach represents a new platform with potential use in biosensors, diagnostics and bioactive layers.

Introduction

The adsorption of proteins onto solid surfaces has been the subject of continuing interest and investigations over recent years due to its applications in many areas such as the medical or food industries [1–5]. Interfacing proteins with metallic substrates precisely, with retention of their biological activity, are critical in a number of fields. For example, biosensor applications using surface plasmon resonance as detection system or biomolecule delivery system using metallic nanoparticles, are promising applications needing a better understanding of the biomolecule (i.e. proteins) surface interactions [6–9].

Unfortunately, such systems are facing problems due, amongst others, to non-specific binding and detection system limitations. Indeed, previous studies have shown that non-specific protein adsorption is a complex phenomenon depending on the substrate surface characteristics, on environmental conditions (pH, ionic strength…) or protein properties (charge, structure, orientation,…) [10–14]. Of particular interest is the effect of protein surface density. Indeed, it was previously demonstrated that molecular recognition efficiency in antigen-antibody complex is decreasing with increasing surface density as a consequence of the combination of steric hindrance and electrostatic effects between proteins and between proteins and surface [15]. It is therefore expected to decrease non-specific binding through minimization of such effects. By the way, recently, Asuri et al. [16] have discovered that the use of curved surfaces enhances protein stability compared to flat surfaces by decreasing the lateral interactions between adjacent molecules. Therefore, one way to avoid or to minimize surface density effect, through minimization of the above-mentioned interactions, would be to use a high density array of metallic clusters, each one designed to immobilize one protein molecule [17]. In this case, gold nanoparticles—AuNPs—appear to be excellent candidates for many reasons: (i) they are relatively inert, (ii) they can be easily functionalized through thiolate groups and (iii) the synthesis of size controlled AuNPs is quite easy and can be tuned to match the selected protein dimensions (5–20 nm).

Concerning detection systems, many methods have been used to study the adsorption and recognition of proteins on

G. Tourillon (✉)
Institut de Recherches sur la Catalyse et l'Environnement – IRCELYON, Université Lyon1, 2 Avenue A.Einstein, 69626 Villeurbanne Cedex, France
e-mail: gerard.tourillon@ircelyon.univ-lyon1.fr

L. Dreesen (✉) · C. Volcke · Y. Sartenaer · P. A. Thiry · A. Peremans
Research Centre in Physics of Matter and Radiation (PMR), FUNDP - University of Namur, rue de Bruxelles, 61, B-5000 Namur, Belgium
e-mail: laurent.dreesen@fundp.ac.be

surfaces including surface plasmon resonance (SPR), fluorescence techniques [18–20], atomic force microscopy (AFM) [21, 22], UV-visible absorption spectroscopy [23, 24], Raman spectroscopy [25, 26] and Fourier transform infrared reflection absorption spectroscopy (FT-IRRAS) [27]. However, these techniques face difficulties in addressing detailed molecular properties of the ad-layer. Hopefully, in recent years, sum-frequency generation vibrational spectroscopy (SFG) has become a very powerful spectroscopic tool for studying surfaces and interfaces [28–31] but also in analysing proteins systems [32–37]. Indeed, SFG is a spectroscopic technique where two laser beams (a visible and an infrared one) are focused on the sample surface. This gives rise to an optical process which generates a third beam at a frequency which is the sum of the frequencies of the incident beams. This spectroscopic tool is very sensitive to inversion symmetry modification occurring at surfaces and interfaces. This particularly interesting characteristic makes it also highly sensitive to molecular conformations. Up to now, despite its applicability to various systems, SFG spectroscopy was mainly applied, except in a few papers [38, 39], to planar geometries. However, recently, Yeganeh et al. [40] demonstrated that the Total Internal Reflection (TIR) configuration reduces the destructive interferences associated with non-linear optical spectroscopy of small particles making possible SFG studies of powders. In a similar way, the SFG spectroscopy in TIR geometry was successfully applied to study the adsorption and oxidation of CO on monolayer films of platinum cubic nanoparticles [41]. Moreover, we have just shown that SFG spectroscopy performed in the TIR configuration provides excellent signal-to-noise ratio and high signal to background ratio compared to the external geometry traditionally used for studying the conformation of adsorbed molecules [42]. Therefore, combining SFG spectroscopy in TIR mode with high-density array of gold nanoparticles is expected to overcome some problems encounter in biomolecular recognition and biosensors applications, i.e. increasing signal-to-noise ratio. In our case, this is done through minimization of non-specific binding and increasing detection system capabilities.

Herein we show, for the first time to the best of our knowledge, that the SFG spectroscopy in TIR geometry, combined with a regular close-packed array of AuNPs, can be used to probe with a high sensitivity the changes in conformation and orientation induced by a molecular recognition process. The interaction of avidin with biocytin has been selected as a model system of ligand–receptor biomolecules because a direct comparison of our results with those already published can easily be done.

Precisely, biocytin ($C_{16}H_{28}N_4O_4S$) is the product of the covalent bonding of biotin (a vitamin H) to the amino group of a lysine ($C_6H_{14}N_2O_2$) residue. Avidin is a tetrameric protein (15800 Da per monomer) which is found as a minor constituent in egg white [43]. Its four binding sites offered to the biocytin are oriented in two opposite directions, two sites facing upward and the other two downward. Hydrogen bonding is mainly responsible for the strong affinity of avidin to biocytin. In order to check the selectivity of the interaction, avidin pre-saturated with biotin and bovine serum albumin (BSA) was also used. BSA (66430 Da) is a protein playing an important role in maintaining the pH value of the blood [44]. It has a heart-shaped structure and a size of about 7 nm. BSA is known for its ability to bind to a wide variety of ligands but has no particular affinity to biocytin. Biocytinilated thiol (BioSH) was used because, like for metallic substrates, the bonding to the AuNPs should proceed through the thiol group and self-assembly is expected.

The SFG data clearly reveal that the BioSH molecules are well aligned normal to the AuNPs surface, whereas structural disorder is observed on a flat one. This difference can be explained by a decrease in the lateral interactions between adjacent biocytin molecules due to the curvature of the nanoparticle surface. The drastic evolutions of the SFG spectra induced after immersion in avidin solution illustrate our ability to detect the recognition of avidin by biocytin. The specificity of the recognition process is confirmed by the fact that no modification of the SFG characteristics is observed after an immersion in bovine serum albumin—BSA—or avidin saturated biotin solutions.

Experimental section

Materials

The following reagents were used: chloroauric acid ($HAuCl_4 \cdot 3H_2O$ 99.999%, Aldrich), trisodium citrate (Aldrich), methanol chromasolv (Aldrich), trichloromethane chromasolv (Aldrich), chlorhydric acid (Aldrich), nitric acid (Aldrich), sulfochromic acid solution (VWR), dodecanethiol (DDT–Aldrich) and aminophenyltrimethoxysilane—APhS (ABCR). Methanol chromasolv was used for washing. Water was Millipore purified with specific resistivity not lower than 18.2 MΩ cm.

Synthesis of dense AuNPs monolayer

The main steps of the AuNPs attachment procedure to an equilateral quartz prism have been described elsewhere [42]. Briefly, the surface of the prism was cleaned by successive immersion in an aqua regea medium and sulfochromic acid solution, then rinced with pure water and dried in N_2 flow. The fresh cleaned surface was covered by an aminophenyltrimethoxysilane—APhS—monolayer and

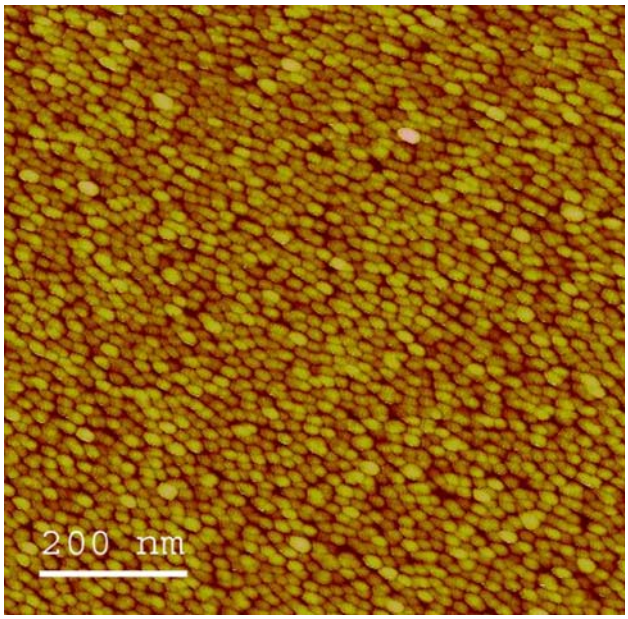

Fig. 1 AFM image of a quartz disc surface covered by an APhS monolayer after immersion for 12 h in a gold colloidal solution, showing the formation of a close-packed AuNPs array on the quartz surface

dipped in a gold nanoparticle suspension for 12 h. The colloidal gold nanoparticles—Au NPs—were prepared by the citrate reduction process, following the method proposed by Frens [45]. The nanoparticles are well spherical with an average size of 11 ± 1 nm as confirmed by TEM. The UV-visible absorption spectra of the AuNPs solution or of a quartz surface coated with AuNPs exhibit a maximum at 520 nm characteristic of the surface plasmon of 10 nm size non-interacting AuNPs [46]. The AFM image (Fig. 1) clearly shows that the citrate-capped negatively charged AuNPs were immobilized onto the amine-terminated surface (through the protonated amine groups) forming a close-packed array of gold nanoparticles which is a key parameter for tailoring the adsorption process of biomolecules. Moreover, the size distribution of the gold nanoparticles deduced from the AFM image is centred at 12.8 ± 2.5 nm (after tip size deconvolution as described elsewhere [47]), which is in very good agreement with that obtained by TEM.

Sample preparation

Biocytinylated thiol (BioSH) is the product of the reaction between biocytin (0.01 M in trifluoroethanol—TFE) and an equimolar amount of 2-iminothiolane hydrochloride (0.01 M in TFE) in the presence of triethylamine for 2 h at room temperature. The AuNPs modified surfaces were immersed in a 10^{-2} M trifluoroethanol (TFE) solution of BioSH for 12 h, rinced with TFE and methanol and dried under N_2 flow. The prism was mounted on a special sample holder and the SFG spectrum was recorded. For the study of the BioSH-protein interaction, the BioSH sample was then immersed for 1 h in a HEPES buffer solution containing one of the three under study proteins (avidin, avidin pre-saturated with biotin, BSA; 10^{-6} M, pH = 7.4), rinsed with the buffer solution and pure water.

SFG setup

A detailed description of the SFG setup can be found elsewhere [48]. Briefly, the infrared and visible laser beams required to perform SFG spectroscopy were generated by two optical parametric oscillators (OPOs) built around $LiNbO_3$ and BBO non-linear crystals, respectively. The infrared OPO was pumped by one-third of the fundamental beam of an all-solid-state Nd: YAG pulsed laser operating at 25 Hz and delivering around 100 single pulses (duration ~12 ps) per laser burst (duration ~1 μs). The infrared beam is tuneable from 2.5 μm to 4.2 μm with an average power of 25 mW and a resolution of 2 cm^{-1}. The remaining part of the fundamental beam generated by the injection laser was frequency-tripled and used to pump the visible OPO. The visible beam was set at 532 nm with an average power of 15 mW and a resolution of 3 cm^{-1}.

The visible and infrared beams (diameters ~1 mm) were p polarized and focused on the base of an equilateral quartz prism in such a way that the angle of incidence of the visible beam is just larger than the quartz critical angle (43°). With this particular value, the infrared incidence angle is close to 50° and therefore both beams are in the total internal reflection conditions. The SFG photons were detected by a photomultiplier tube after spatial and spectral filtering by means of Raman filters and a double-grating monochromator.

Results and discussion

The TIR-SFG characteristics in the C–H vibration domain of the close-packed array of AuNPs and of BioSH molecules adsorbed on this array are presented in Fig. 2 curve a and curve b, respectively.

The spectrum of the AuNPs array (Fig. 2 curve a) is completely flat, evidencing no vibration contribution at all in contrast to that of BioSH (Fig. 2 curve b) which is composed of four main peaks (labelled A, B, C and D) located at 2882, 2942, 2975 and 3079 cm^{-1} and of one shoulder (E) at 2859 cm^{-1}, respectively. The latter can be assigned to the symmetric methylene stretching vibration mode coming from the CH_2 groups along the molecular chain [49] and should be associated to the asymmetric

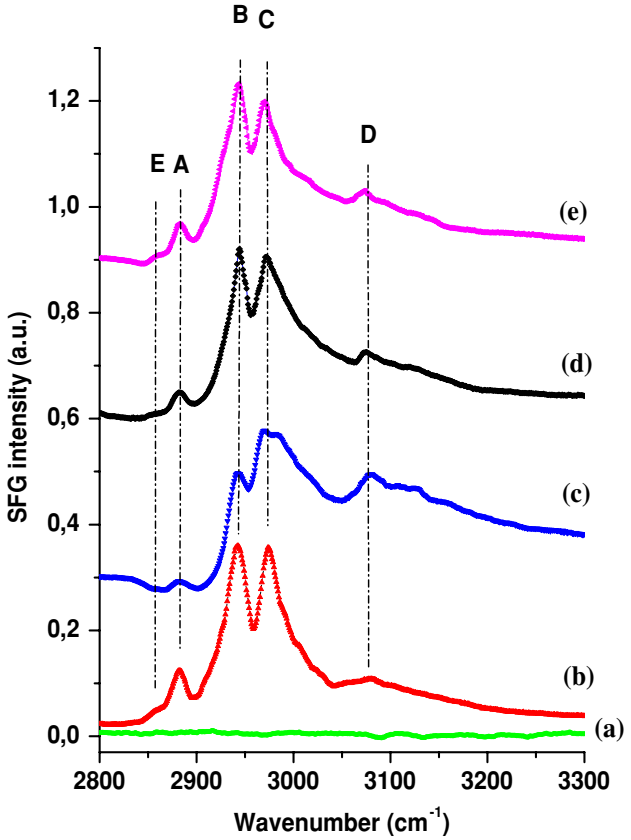

Fig. 2 TIR-SFG spectra of a close-packed array of AuNPs (a), BioSH molecules adsorbed on AuNPs before (b) and after immersion in an avidin solution (c), pre-saturated avidin (d) and BSA (e). The spectra c, d and e have been shifted each by an offset of 0.3 from spectrum b, for clarity. For the assignment of the vibration bands, see the text

stretch expected around 2917 cm^{-1} that is hardly observable on Fig. 2. For a perfectly ordered chain, the methylene groups are in an "all trans" conformation and thus symmetrically distributed along the longitudinal axis of the molecule. They should therefore be SFG inactive. The very low intensity of band E demonstrates that the molecules are well organized on the AuNPs, being oriented close to the normal of the surface. The CH bands, labelled A and B, are assigned to the symmetric and asymmetric stretching vibrations of the single CH_2 group of the tetrahydrothiophene ring. Their higher frequency values compared to those of the methylene groups of the chain are due to the strain induced by the ring structure [50], in good agreement with the results obtained for biocytin molecules adsorbed on a CaF_2 prism [51]. The other vibration, labelled C, is related to the stretching mode of the two CH bonds attached to the tetrahydrothiophene ring [52–54]. Finally, the last broad structure at 3079 cm^{-1}, labelled D, could be associated to a Fermi resonance-enhanced overtone of the 1550 cm^{-1} band coming from the amide II entities [50]. The detection of the CH vibration modes of the tetrahydrothiophene ring confirms that the BioSH molecules are anchored normal to the AuNP surface in such a way that the vibrations of the CH bonds located on the ring have non-vanishing dynamic dipole components perpendicular to the surface, being thus SFG active.

The SFG measurements are indicative of the building of a well ordered self-assembled ad-layer on the close-packed array of AuNPs. This is indeed in great contrast with the results obtained on flat metallic surfaces [55] or on a CaF_2 substrate [51] where chain disorder was observed, especially on Au, Pt and Ag surfaces. Two plausible explanations may be put forward to explain these differences. The first one is that structural defects in the ad-layer are generated by the interactions of multiple functional groups of BioSH with the flat metallic surface, which is disfavoured on a curved AuNP one. The second hypothesis is that lateral interactions between adjacent adsorbed molecules induce modifications in the molecular conformation, which are suppressed on highly curved substrates. If BioSH-surface interaction is the main parameter, the recognition process of BioSH for avidin should not be observed on a flat substrate which is evidently not the case [51, 55]. On the contrary, varying the distance between two gold nanoparticles during the attachment process, just by changing the immersion time of the prism in the AuNPs solution, should enhance or disfavour the lateral interactions. A well oriented BioSH ad-layer is obtained on a close-packed array of AuNPs (shown before) while structural disorder is observed on a low coverage one (data not shown).This phenomenon can be understood by considering the size of the metallic nanoparticle and the size of the BioSH molecule which are in both cases in the range of a few nanometre. By tailoring the lateral distance of the close-packed array of AuNPs, one BioSH molecule can match one nanoparticle, minimizing the lateral BioSH–BioSH interactions.

After immersion in an avidin solution (10^{-6} M; HEPES buffer), the SFG spectrum undergoes drastic modifications as illustrated in Fig. 2 curve c. The intensity of bands A, B and C, directly connected to the CH and CH_2 vibrations of the tetrahydrothiophene ring, is greatly reduced which can be viewed as a reorganisation of the BioSH conformation in order to match the bonding pocket of the avidin. The interaction between the two biological species through hydrogen bonding should induce a change in the tilt angle of the ring, leaving the CH and CH_2 bonds more parallel to the AuNP surface and consequently, SFG inactive. On the contrary, the intensity of band D, associated to a Fermi resonance-enhanced overtone of the 1550 cm^{-1} band coming from the amide II entities, increases due to the reorientation process during the recognition process of avidin by the BioSH ad-layer. The band E connected to the

methylene groups is quite similar to those observed before the immersion treatment. These characteristics clearly indicate that the BioSH molecular chains are still oriented normal to the AuNP surface when the apex ring has to change its conformation for matching the bonding pocket of avidin. Finally, we notice an increase in the SFG non-resonant part which could be due to the electronic properties of avidin and/or to water molecules inside the layer. An unambiguous assignment of this non-resonant part is difficult and requires calculations which are out of the scope of this study. To address the specificity of the molecular recognition by TIR-SFG, we performed two other experiments. The first one consists of immersing the BioSH layer in an avidin pre-saturated with biotin solution (10^{-6} M, HEPES buffer). In this case, the four binding pockets are blocked by biotin, making them insensitive to further interactions with the adsorbed BioSH molecules. The second experiment consists of an immersion in a BSA solution (10^{-6} M, HEPES buffer). The SFG spectra corresponding to both experiments are displayed in Fig. 2 curve d and curve e, respectively. These spectra reveal the same main features as those obtained in Fig. 2 curve b, recorded previously to any treatment attesting the specificity of the process.

Conclusions

In conclusion, we have shown that the sum frequency generation spectroscopy in total internal reflection (TIR-SFG) is a powerful tool for probing, without target amplification or the use of markers, the changes in conformation and orientation induced by the recognition process of avidin by BioSH molecules adsorbed on AuNPs. Two main parameters play a crucial role in getting SFG data with an excellent signal-to-noise ratio and high sensitivity: (i) the TIR geometry and (ii) the use of a regular close-packed array of AuNPs. The TIR geometry, by reducing the destructive interferences associated with non-linear optical spectroscopy of small particles [35], increases the SFG signal by at least a factor to 15 compared to the reflection geometry, consequently the detection level is 10 times higher than that of the "classical" configuration. The second key parameter concerns the use of AuNPs, highly curved substrate, which minimizes the lateral interactions between adjacent adsorbed biomolecules and thus leads to their deactivation. Moreover by tailoring the size and the lateral distance of the AuNPs arranged in a close-packed array, one protein molecule can match one nanoparticle leading to self-assembling of the protein layer. Another interest of AuNPs for SFG spectroscopy, using a 532 nm visible laser beam, comes from their very low contribution to the non-resonant background in comparison to a flat gold surface which induces quite frequently destructive interferences with the vibrational resonances [56], making difficult the studies of adsorbed molecules. This difference is directly connected to the specific electronic properties of each surface: electrons from the d band of the flat gold surface can be optically excited which is not the case with the AuNPs (maximum of absorption at $\sim$528 nm). SFG experiments at different visible wavelengths are under way to precise these phenomena. Our experimental results suggest that the observed enhancements in protein organization, recognition process and stability are not restricted to AuNPs but should be common to nanomaterials as already obtained with single wall carbon nanotubes (SWNTs) [16]. The association of the TIR-SFG spectroscopy with a regular close-packed array of nanoparticles (or nanomaterials) represents a new platform with potential use in biosensors, diagnostics and bioactive layers.

Acknowledgements L.D. and C.V. acknowledge the Walloon Region and the University of Namur—FUNDP for financial supports. C.V. is a postdoctoral researcher of the Belgian Fund for Scientific Research (F.R.S.-F.N.R.S.). This study was supported by the Centre National de la Recherche Scientifique (C.N.R.S.) and by the Belgian Fund for Scientific Research (F.R.F.C.).

References

1. Horbett TA, Brash JL (1995) Proteins at interfaces II, fundamentals and applications. ACS Symp. Ser.602. American Chemical Society, Washington, DC
2. Brash JL, Horbett TA (1975) Proteins at interfaces, physicochemical and biochemical studies. American Chemical Society, Washingthon, DC
3. Norde W, Lyklema J (1991) J Biomater Sci Polym Ed 2:183
4. Ramsden JJ (1994) Q Rev Biophys 27:41
5. Dickinson E (1989) Colloids Surf 42:191
6. Barone PW, Baik S, Heller DA, Strano MS (2005) Nat Mater 4:86
7. Chen RJ, Bangsaruntip S, Drouvalakis KA, Kam NWS, Shim M, Li Y, Kim W, Utz PJ, Dai H (2003) Proc Natl Acad Sci USA 100:4984
8. Kam NWS, Jessop TS, Wender PA, Dai HJ (2004) J Am Chem Soc 126:6850
9. Graff RA, Swanson JP, Barone PW, Baik S, Heller DA, Strano MS (2005) Adv Mater 17:980
10. Norde W, Giacomelli CE (1999) Macromol Symp 145:125
11. Norde W (1995) Cell Mater 5:97
12. Sethuraman A, Han M, Kane RS, Belfort G (2004) Langmuir 20:7779
13. Xu L-C, Siedlecki CA (2007) Biomaterials 28:3273
14. Lu JR, Zhao XB, Yaseen M (2007) Curr Opin Colloid Interface Sci 12:9
15. Xu H, Lu JR, Williams DE (2006) J Phys Chem B 110:1907
16. Asuri P, Karajanagi SS, Yang H, Yim TJ, Kane RS, Dordick JS (2006) Langmuir 22:5833
17. Leung C, Xirouchaki C, Berovic N, Palmer RE (2004) Adv Mater 16:223
18. Lahav M, Vaskevich A, Rubinstein I (2004) Langmuir 20:7365
19. Häusling L, Ringsdorf H, Schmitt FJ, Knoll W (1991) Langmuir 7:1837

20. Ramdas L, Zhang W (2002) Biophotonics 9:342
21. De Paris R, Strunz T, Oroszlan K, Güntherodt HJ, Hegner M (2000) Single Mol 1:285
22. Lo YS, Huefner ND, Chan WS, Steven F, Harris JM, Beebe TP Jr (1999) Langmuir 15:1373
23. Sastry M, Lala N, Patil V, Chavan SP, Chittiboyina AG (1998) Langmuir 14:4138
24. Lala N, Chittiboyina AG, Chavan SP, Sastry M (2002) Coll Surf A 205:15
25. Clarkson J, Sudworth C, Masca SI, Batchelder DN, Smith DA (2000) J Raman Spectrosc 31:373
26. Torreggiani A, Fini G (1999) J Mol Struct 480–481:459
27. Pradier CM, Salmain M, Zheng L, Jaouen G (2002) Surf Sci 502–503:193
28. Shen YR (1989) Annu Rev Phys Chem 40:327
29. Gracias DH, Chen Z, Shen YR, Somorjai GA (1999) Acc Chem Res 32:930
30. Tadjeddine A, Peremans A (1998) Spectroscopy for surface science, chap 4. Wiley, New York
31. Williams CT, Yang Y, Bain CD (2000) Langmuir 16:2343
32. Dreesen L, Humbert C, Hollander P, Mani AA, Ataka K, Thiry PA, Peremans A (2001) Chem Phys Lett 333:327
33. Wang J, Even MA, Chen X, Schmaier AH, Waite JH, Chen Z (2003) J Am Chem Soc 125:9914
34. Wang J, Clarke ML, Zhang Y, Chen Z (2003) Langmuir 19:7862
35. Kim J, Somorjai GA (2003) J Am Chem Soc 125:3150
36. Mermut O, Phillips DC, York RL, McCrea KR, Ward RS, Somorjai GA (2006) J Am Chem Soc 128:3598
37. Wang J, Clarke ML, Chen X, Even MA, Johnson WC, Chen Z (2005) Surf Sci 587:1
38. Humbert C, Busson B, Abid JP, Six C, Girault HH, Tadjeddine A (2005) Electrochim Acta 50:3101
39. Weeraman C, Yatawara AK, Bordenyuk AN, Benderskii AV (2006) J Am Chem Soc 128:14244
40. Yeganeh MS, Dougal SM, Silbernagel BG (2006) Langmuir 22:637
41. Kweskin SJ, Rioux RM, Habas SE, Komvopoulos K, Yang P, Somorjai GA (2006) J Phys Chem B 110:15920
42. Tourillon G, Dreesen L, Volcke C, Sartenaer Y, Thiry PA, Peremans A (2007) Nanotechnology 18:415301
43. Pugliese L, Coda A, Malcovati M, Bolognesi M (1993) J Mol Biol 231:698
44. Carter DC, Ho JX (1994) Adv Protein Chem 45:153
45. Frens G (1973) Nature 241:20
46. Rosei R, Lynch DW (1972) Phys Rev B 5:3883
47. Rasa M, Kuipers BWM, Philipse AP (2002) J Colloid Interf Sci 250:303
48. Mani AA, Dreesen L, Humbert C, Hollander P, Caudano Y, Thiry PA, Peremans A (2002) Surf Sci 502–503:261
49. Bain CD (1995) J Chem Soc Faraday Trans 91:1281
50. Lin-Vien D, Colthup NB, Fateley WG, Grasselli JG (1991) The handbook of infrared and raman characteristic frequencies of organic molecules. Academic Press, San Diego, CA
51. Dreesen L, Sartenaer Y, Humbert C, Mani AA, Methivier C, Pradier CM, Thiry PA, Peremans A (2004) Chem Phys Chem 5:1719
52. Ji N, Shen YR (2004) J Chem Phys 120:7107
53. Lu RL, Gan W, Wu B-H, Zhang Z, Guo Y, Wang H-F (2005) J Phys Chem B 109:14118
54. Polavarapu PL, Smith HE (1988) J Phys Chem 92:1774
55. Dreesen L, Sartenaer Y, Humbert C, Mani AA, Lemaire LL, Methivier C, Pradier CM, Thiry PA, Peremans A (2004) Thin Solid Films 464–465:373
56. Dreesen L, Humbert C, Celebi M, Lemaire JJ, Mani AA, Thiry PA, Peremans A (2002) Appl Phys B 74:621